

Article

Micro-Structural Design of CoFe₂O₄/SWCNTs Composites for Enhanced Electromagnetic Properties

Zaoxia Hou^{1,2,3}, Chenyang Liu^{1,2,3}, Jialuo Gong^{1,2,3}, Junjie Wu⁴, Shuchen Sun^{5,*}, Mu Zhang^{1,2,3,*} and Xudong Sun^{1,2,3,*}

¹ Key Laboratory for Anisotropy and Texture of Materials (Ministry of Education), Northeastern University, Shenyang 110819, China

² School of Materials Science and Engineering, Northeastern University, Shenyang 110819, China

³ Foshan Graduate School of Innovation, Northeastern University, Foshan 528311, China

⁴ Sinosteel Engineering & Technology (Inner Mongolia) Co., Ltd., Baotou 014000, China

⁵ School of Metallurgy, Northeastern University, Shenyang 110819, China

* Correspondence: sunsc@smm.neu.edu.cn (S.S.); zhangm@mail.neu.edu.cn (M.Z.); xdsun@mail.neu.edu.cn (X.S.)

Abstract: In order to prepare microwave-absorbing materials with low density and high wave absorption performance, CoFe₂O₄/SWCNTs composites with well-designed necklace-like structures were successfully prepared in this paper by a simple solvothermal method. CoFe₂O₄/SWCNTs composites with different cobalt salt contents were synthesized by adjusting the experimental parameters. The results of the relative complex permeability and relative permittivity of the samples, which were investigated by vector network analysis in the frequency range of 2 to 18 GHz, are collected to support the study of the microwave absorption characteristics of the samples. Different microsphere densities and different cobalt salt contents have obvious differences in the electromagnetic absorption properties of the composites. When the additions of FeCl₃·6H₂O, Co(Ac)₂·4H₂O, and NH₄Ac were 0.432, 0.200, and 0.400 g, respectively, the best reflection loss reached −42.07 dB, and the effective absorption frequency (RL < −10 dB) ranges from 3.2 to 18 GHz. Therefore, this is a preparation strategy of CoFe₂O₄/SWCNTs composites with necklace structure, which has the advantages of simple process, environmental friendliness, low cost, and high stability. The unique necklace-like structure design makes the carbon nanotubes partially exposed, which is more beneficial to achieve good impedance matching and giving the CoFe₂O₄/SWCNTs composite excellent electromagnetic loss capability.

Keywords: CoFe₂O₄/SWCNTs composites; microwave absorption; necklace-like structure; double loss mechanism; impedance matching



Citation: Hou, Z.; Liu, C.; Gong, J.; Wu, J.; Sun, S.; Zhang, M.; Sun, X. Micro-Structural Design of CoFe₂O₄/SWCNTs Composites for Enhanced Electromagnetic Properties. *Coatings* **2022**, *12*, 1532. <https://doi.org/10.3390/coatings12101532>

Academic Editor: Stefan Ioan Voicu

Received: 24 August 2022

Accepted: 29 September 2022

Published: 13 October 2022

Publisher's Note: MDPI stays neutral with regard to jurisdictional claims in published maps and institutional affiliations.



Copyright: © 2022 by the authors. Licensee MDPI, Basel, Switzerland. This article is an open access article distributed under the terms and conditions of the Creative Commons Attribution (CC BY) license (<https://creativecommons.org/licenses/by/4.0/>).

1. Introduction

Nowadays, with the rapid development and broad application of electronic devices and wireless communication technologies, electromagnetic radiation poses a serious threat to human health and the regular operation of electronic devices and has become another major problem after air, water, and noise pollution [1–4]. To solve the problem of electromagnetic radiation pollution, absorbing materials that can absorb and attenuate incident electromagnetic waves and convert the incident electromagnetic energy into heat-based energy to be consumed are attracting much attention [5]. There are many materials for radiation protection, such as glasses based on TeO₂-WO₃-Bi₂O₃-MoO₃-SiO [6], while this paper focuses on carbon nanotube-based microwave-absorbing composites. Therefore, the research and development of high-performance absorbing materials to solve the electromagnetic pollution problem are urgent [7]. According to the research progress of absorbing materials, using the excellent properties of composite absorbing materials with different components to make materials with both magnetic loss and electrical loss will become the future requirements and development direction of absorbing materials.

Carbon materials have been recognized and widely used in the microwave absorption field [8–10]. It is well known that carbon nanotubes are one of the significant carbon materials in the field of electromagnetic absorption [11,12] and one of the crucial materials in the field of military wave-absorbing stealth technology and civil electromagnetic protection [13]. Wu et al. [14] synthesized three-dimensional porous CuS@rGO composite aerogels with MA properties and IR stealth capability by hydrothermal and ascorbic acid thermal reduction methods and subsequent freeze-drying techniques. Peymanfar et al. [15,16] dissected carbon-based biomass-derived materials used as microwave-absorbing structures and provided a new idea of immobilizing oxygen-containing functional groups in carbon-based structures. Carbon nanotubes (CNTs) have attracted extensive attention as microwave absorbers due to their low density and good electrical conductivity [17,18]. However, because carbon nanotubes have strong electrical conductivity [19], large complex dielectric constant [20–22], small permeability, and low magnetic loss, they mainly attenuate electromagnetic waves through dielectric loss, which is difficult to match with free space, resulting in poor impedance matching characteristics and less than ideal electromagnetic absorption performance [23,24]. To improve impedance matching and microwave absorption performance, the preparation of carbon nanotubes compounded with other materials is an effective method. However, the disadvantage of ferric oxide (Fe_3O_4) is that the high-frequency band absorption effect is not ideal, the density is larger [25–27], so it is not good enough to achieve the “thin, light, wide, strong” requirements of the new absorbing material. Spinel-type cobalt ferrite is a kind of spinel-type ferrite with excellent performance, which has medium saturation magnetization strength, excellent chemical stability, high coercivity, strong wear anisotropy, high mechanical strength, and large magnet crystal anisotropy constant, so it has a wide range of applications in rechargeable batteries, high-density magnetic recording, biomedicine and other fields [28]. At the same time, cobalt ferrite is also a good electromagnetic wave-absorbing material, which enhances the effect on electromagnetic waves due to its many pores, and has received wide attention from scholars in the field of microwave absorption [29,30]. Fu et al. [31] prepared a new CoFe_2O_4 hollow sphere/graphene composite using a facile vapor diffusion method in combination with calcination at 550 °C. The composite achieved a minimum reflection loss value of -18.58 dB at 12.9 GHz and effective absorption bandwidth of 3.7 GHz when the thickness is 2 mm. Luo et al. [32] successfully prepared layered CoFe_2O_4 /CNTs/WPU composite aerogels using a facile directional freeze-drying method. The best microwave absorption performance of the heterogeneous aerogel reached -45.8 dB at 11.68 GHz when the matched thickness was 6.8 mm. Zhang et al. [33] used a vapor diffusion method in combination with calcination to synthesize olive sphere-shaped CoFe_2O_4 particles assembled from nanoparticle layers showing a porous structure, and the minimum RL value of CoFe_2O_4 olive spheres with a thickness of 2.5 mm reached -34.1 dB and an effective absorption bandwidth of 2.6 GHz. Wu et al. [34] synthesized core/shell structured nanocomposites with carbon nanotubes (CNTs) as the core and CoFe_2O_4 nanoparticles as the shell by a one-step hydrothermal method, matching the min RL value is -49.96 dB when a thickness dm value is 3.18 mm and the best absorption bandwidth of 4.40 GHz when the dm value is 1.64 mm. In summary, the composite material of cobalt ferrite and carbon material is one of the most popular electromagnetic wave-absorbing materials at present. However, there are still some problems, including the complicated preparation method and the poor matching thickness of the material. Therefore, we design a composite wave-absorbing material of CoFe_2O_4 and carbon nanotubes with simple preparation and a unique necklace-like structure.

Morphology, phase, and defects also play a significant role in microwave absorption. Peymanfar et al. [35] investigate the microwave absorption properties of graphitic carbon nitride based on structure and defects. Chen et al. [36] found a competitive and cooperative relationship between conduction loss, interfaces, and defects. The solvothermal method of preparation is characterized by particle formation through the dissolution and crystallization process, which is characterized by high purity, good dispersion, complete

grain development, and controllable size. Because of these advantages of the solvothermal method, it is better to control the microstructure of the sample and thus adjust the electromagnetic parameters of the microwave absorber.

In order to meet the requirements of lightweight and thin thickness, a simple solvothermal method is chosen to prepare CoFe₂O₄/SWCNTs composites in this paper, and necklace-like CoFe₂O₄/SWCNTs composites with dual dielectric and magnetic losses are successfully prepared. Due to the synergistic effect of the magnetic loss capacity of CoFe₂O₄ and the dielectric loss capacity of SWCNTs, as well as the multiple scattering attenuation effects of the 3D lattice necklace-like structure on electromagnetic waves, the composites exhibit good wave absorption performance. The minimum RL value reaches -42.07 dB, the EABD reaches 3.8 GHz, and the thickness range is 1–5 mm. This method is simple and easy to implement and provides an effective way to develop high-performance MAM.

2. Materials and Methods

2.1. Chemicals

All reagents applied in this experiment were analytical grade. Ferric chloride (FeCl₃·6H₂O, 99.0%) hexahydrate, cobalt acetate (Co(Ac)₂·4H₂O, 99.5%) tetrahydrate, ammonium acetate (NH₄Ac), and ethylene glycol were from Shanghai Sinopharm Group Chemical Reagent Co. The carbon nanotubes used to prepare the necklace structured CoFe₂O₄/SWCNTs composites were from Nanjing Xianfeng Nanomaterial Technology Co. Ltd. (Nanjing, China). The deionized water used in all experiments was from Milli-Q system (Millipore, Bedford, MA, USA).

2.2. Functionalization of Single-Walled Carbon Nanotubes

After acid treatment, the number of functional groups on the surface of carbon nanotubes increases, making them more suitable for accepting other nanoparticles on their surface growth. A typical acidification process is as follows, 200 mg of carbon nanotubes are added to a three-necked flask containing a mixture of concentrated nitric acid and concentrated sulfuric acid (volume ratio: 3:1). The above mixture was dispersed by continuous strong sonication for 3 h. When the carbon nanotubes were completely dispersed, the three-neck flask was placed in an oil bath, heated to 80 °C, and maintained at that constant temperature for 1 h. Then the acidified carbon nanotubes were cooled to room temperature and left to stand in deionized water for 12 h. The rested carbon nanotubes were rinsed to neutral (PH ≈ 7) by filtration with a large amount of deionized water and dried at 60 °C in an oven for 8 h. The functionalized carbon nanotubes are ready for subsequent use.

2.3. Preparation of CoFe₂O₄/SWCNTs Necklace-like Structure

0.54 g FeCl₃·6H₂O, 0.25 g Co(Ac)₂·4H₂O, and 0.50 g NH₄Ac were dissolved in 60 mL EG. After the solution was completely dissolved, different contents of functionalized SWCNTs were weighed and added to the light yellow solution, then sonicated continuously for 3 h. After the SWCNTs were well dispersed, small magnets were added and stirred for 30 min. Then the solution was poured into a 100 mL Teflon-lined stainless autoclave and held in an oven at 200 °C for 24 h. The samples were removed and washed with deionized water and ethanol 3 times, respectively. Vacuum drying was conducted at 60 °C for 8 h.

The experimental parameters (cobalt salt gradient (0.2 g, 0.25 g, 0.3 g, 0.35 g as Co-1, Co-2, Co-3, Co-4) where carbon nanotubes were 4 mg) were adjusted to achieve the modulation of the microstructure of spinel ferrites, to investigate the effect of micro-structural changes on the absorbing properties of the samples. The cobalt and iron salts were varied together, and they were added in multiples of 0.8, 1, 1.2, and 1.4 based on 0.25 g of cobalt salt and 0.54 g of iron salt as a reference. Finally, the stoichiometry of the cobalt salt was chosen as the standard to differentiate the four samples. The ratio of cobalt salt to iron salt did not change; what changed was the amount added. By adjusting the ratio of cobalt salts, it is the amount of cobalt and iron salts added that adjusts the microstructure of the material

2.4. Characterization

The crystal structure and phase composition of CoFe₂O₄/SWCNTs composites were characterized by an X-ray diffractometer (XRD, Model Smartlab 9, Tokyo, Japan) with a Cu K α source (40 KV, 200 mA). Scanning electron microscopy (SEM, JSM-7001F, Tokyo, Japan) and transmission electron microscopy (TEM, JEM-2100F, Tokyo, Japan) were used to analyze the morphology and structure of the CoFe₂O₄/SWCNTs nanomaterials. The composition and distribution of chemical elements on the surface of the samples were investigated by X-ray photoelectron spectroscopy (XPS, Kratos, Manchester, U.K.). The magnetic hysteresis loops were measured by a vibrating sample magnetometer (VSM, Lake Shore Cryotronics, Westerville, OH, USA) at room temperature.

2.5. Characterization of Absorption Properties

The relative complex permeability and relative permittivity of the samples were tested by vector network analysis (VNA, Agilent N5234A, California, CA, USA) in the frequency range of 2 to 18 GHz. The sample powder was miscible with paraffin wax in the mass ratio of 3:7 at 80 °C. The miscible material is quickly poured into a hollow cylindrical mold with an outer diameter of 7 mm, an inner diameter of 3 mm, and a thickness was about 3 mm.

3. Results and Discussion

We successfully synthesized necklace-like CoFe₂O₄/SWCNTs composite heterostructures by a simple solvothermal method using functionalized carbon nanotubes as raw materials, and the schematic illustration of the synthesis strategy of CoFe₂O₄/SWCNTs composites is shown in Figure 1.



Figure 1. Schematic illustration of synthesis strategy for CoFe₂O₄/SWCNTs composites.

First, when CNTs were treated with acid, some negatively charged oxygen-containing functional groups were produced, which provide sites for the growth of CoFe₂O₄ grains. Then, the oxygen-containing functional groups were used as nucleation centers, which are firmly bonded with carbon nanotubes to form a necklace-like composite structure. The specific process in the solvent heat is that when the carbon nanotubes are completely dispersed in the EG solution, Co²⁺ and Fe³⁺ in the solution can be fixed on the surface of single-walled carbon nanotubes by electrostatic adsorption. During the solvothermal process, EG can be dehydrated to generate H₂O in a sealed autoclave under high temperature and pressure. Then an alkaline environment is created by hydrolysis of NH₄AC. Finally, cobalt and iron salts react with OH[−] to form cobalt ferrite (Co²⁺ + 2Fe³⁺ + 8OH[−] → CoFe₂O₄ + 4H₂O) [37,38]. Thus, necklace-like CoFe₂O₄/SWCNTs composites are formed, with CoFe₂O₄ nanoparticles passing through and immobilizing on the CNTs surface.

The phase composition and structure of the necklace-like CoFe₂O₄/SWCNTs composites were investigated by XRD, as shown in Figure 2. All the diffraction peaks obtained were in accordance with the CoFe₂O₄ standard card (JCPDS No. 22-1086). The diffraction peaks were clear and intense, and no obvious impurity peaks were observed, which indicated that the CoFe₂O₄/SWCNTs composite has good crystallization and high purity. In

addition, the diffraction peaks of $\text{CoFe}_2\text{O}_4/\text{SWCNTs}$ composites are almost consistent with the CoFe_2O_4 standard card, which indicates that it is an amorphous structure with little SWCNTs content.

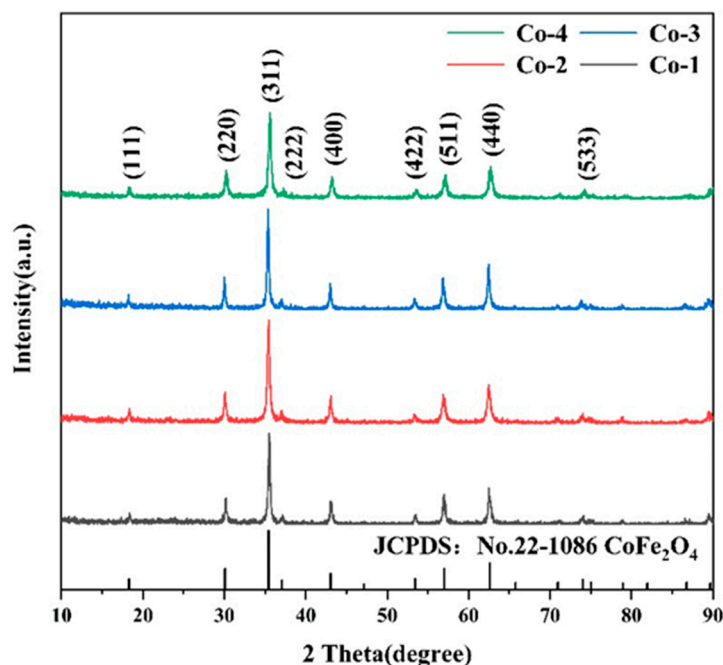


Figure 2. XRD patterns of $\text{CoFe}_2\text{O}_4/\text{SWCNTs}$ composites prepared under different experimental parameters.

The microscopic morphology of the $\text{CoFe}_2\text{O}_4/\text{SWCNTs}$ composites was characterized using SEM, and the morphology of the sample under the cobalt salt gradient is shown in Figure 3. The sample is composed of spherical nanoclusters and cylindrical carbon nanotubes, and the nanospheres wrap around the carbon nanotubes to form a necklace-like structure. SEM of Figure 3a–d clearly shows that the number and distribution density of spherical CoFe_2O_4 clusters obtained by adding different amounts of cobalt salts are significantly different at a carbon nanotube content of 4 mg. With the gradual increase in the cobalt salt content, the number of CoFe_2O_4 microspheres increases, and the spheres become more uniform in size but with little change in size. It is not difficult to understand that the increase in cobalt salt concentration will produce more CoFe_2O_4 microsphere nanocrystals and increase the loading capacity of CoFe_2O_4 microspheres on the surface of single-walled carbon nanotubes, the interface in the material increases, and the necklace-like structures pile up with each other to form a network. It provides the conditions for improving wave absorption performance.

The morphology and structure of the $\text{CoFe}_2\text{O}_4/\text{SWCNTs}$ composites were further characterized by TEM, and the results are shown in Figure 4. As can be observed from Figure 4a, the CoFe_2O_4 microspheres with diameters of about 100–200 nm are uniformly anchored on SWCNTs, and the necklace-like structure of the composite is consistent with the SEM image. In addition, the HRTEM image of Figure 4b shows a lattice spacing of about 0.25 nm and 0.17 nm, which is attributed to the (311) and (422) crystal plane of spinel cobalt ferrite, further confirming the presence of CoFe_2O_4 . The SAED pattern of Figure 4c reveals the polycrystalline structure of the $\text{CoFe}_2\text{O}_4/\text{SWCNTs}$ composite.

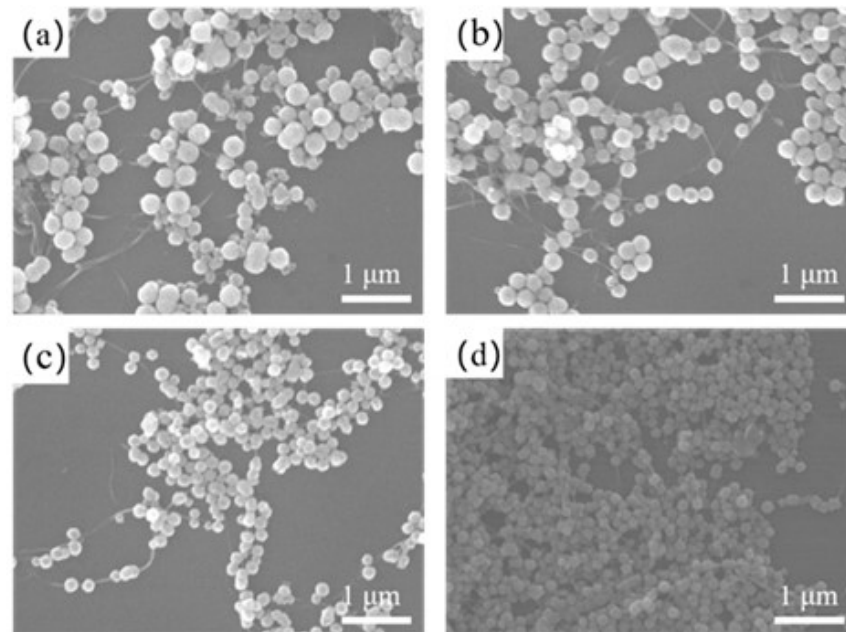


Figure 3. SEM images of $\text{CoFe}_2\text{O}_4/\text{SWCNTs}$ composites under Co salt gradient: (a) Co-1, (b) Co-2, (c) Co-3, (d) Co-4.

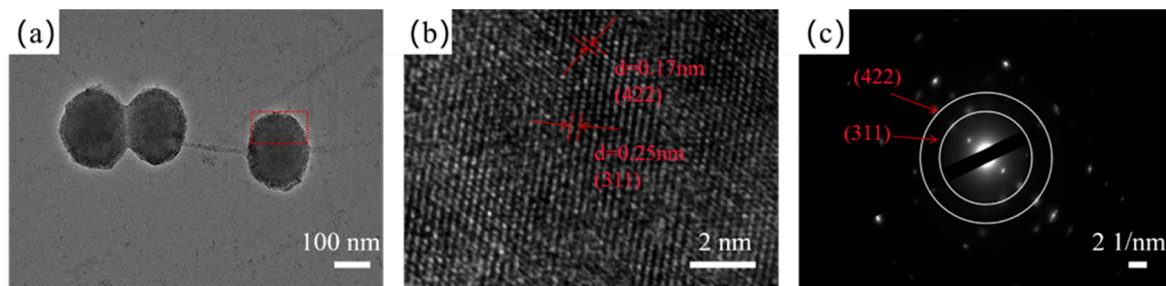


Figure 4. (a) TEM image of $\text{CoFe}_2\text{O}_4/\text{SWCNTs}$, (b) HRTEM image of $\text{CoFe}_2\text{O}_4/\text{SWCNTs}$ and (c) selected area electron diffraction (SAED) image of $\text{CoFe}_2\text{O}_4/\text{SWCNTs}$.

To further investigate the chemical composition and bonding of the $\text{CoFe}_2\text{O}_4/\text{SWCNTs}$ composites, XPS characterization was performed, as shown in Figure 5. All binding energies were normalized concerning C 1s at 284.8 eV. It can be clearly observed from the full spectrum in Figure 5a that there are four elements present, Co, Fe, O, and C, respectively. Figure 5b demonstrates the high-resolution Co 2p spectra, where the peaks at 781.2 eV and 796.8 eV are attributed to the $\text{Co}^{2+} 2p_{3/2}$ and $\text{Co}^{2+} 2p_{1/2}$ spectra, respectively [39,40]. The double-peaked signals at about 786.3 eV and 803.2 eV are assigned to the two oscillating satellites. Thus, the high-resolution XPS spectra of Co 2p indicate the presence of Co^{2+} ions. The Fe 2p spectra of the $\text{CoFe}_2\text{O}_4/\text{SWCNTs}$ composites are shown in Figure 5c. The peaks at 724.4 and 711.2 eV correspond to the binding energies of $\text{Fe}^{3+} 2p_{1/2}$ and $\text{Fe}^{3+} 2p_{3/2}$, respectively, with the oscillating satellites located at 714.8 eV [41]. The detected Co 2p and Fe 2p photoelectron peaks are consistent with the reported peaks of Co^{2+} and Fe^{3+} in CoFe_2O_4 . In Figure 5d, the O 1s spectrum is divided into three parts. The peak at 533.0 eV can be attributed to the adsorbed water. The two peaks located at 531.5 and 530.4 eV are consistent with oxygen in the defect and metal-oxygen bonds, respectively [42].

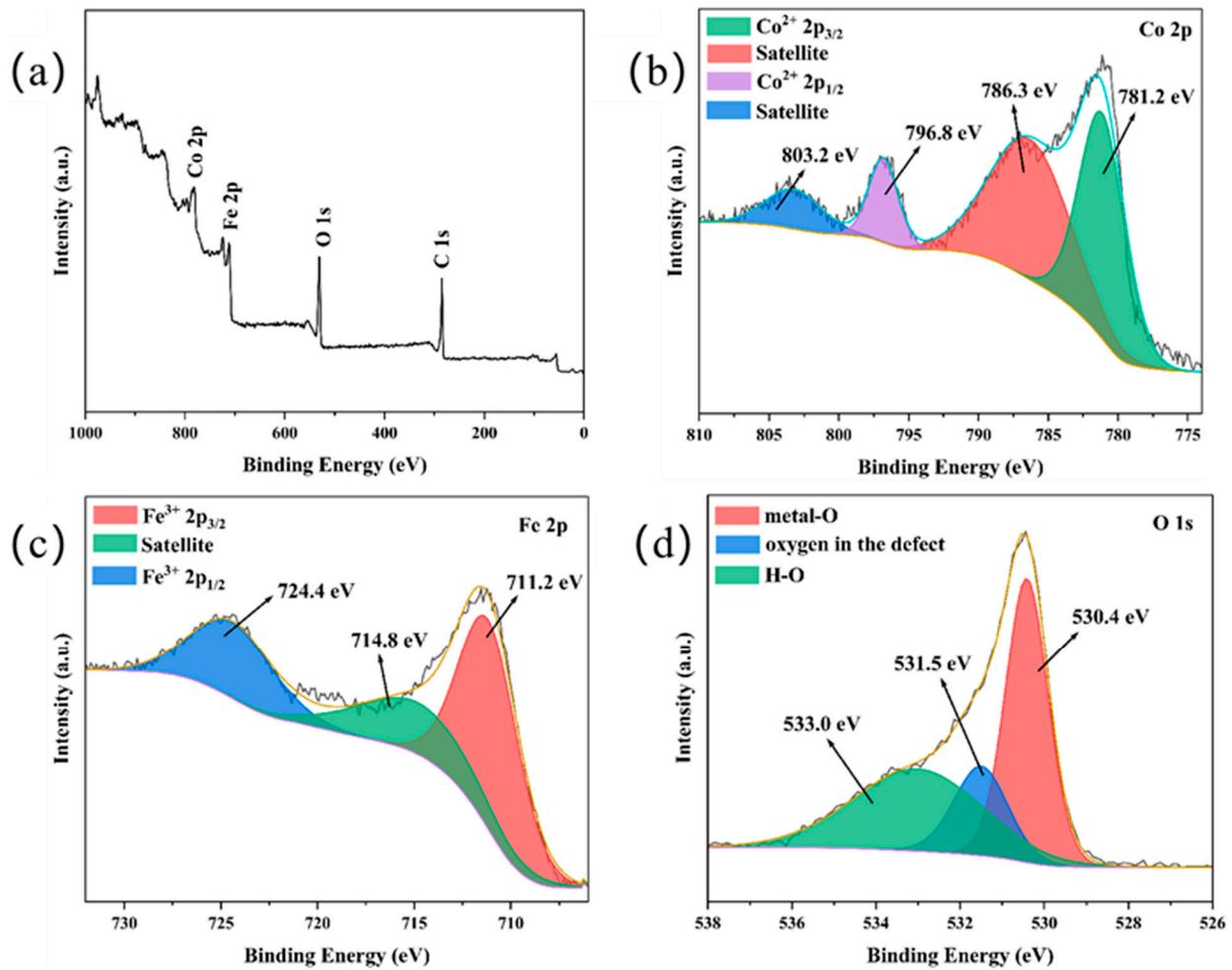


Figure 5. XPS spectra of CoFe₂O₄/SWCNTs composites: (a) full spectrum, (b) Co 2p, (c) Fe 2p, and (d) O 1s.

With the above analysis, we believe that the necklace-like CoFe₂O₄/SWCNTs nanocomposites have been successfully prepared. Next, we compared and analyzed the wave absorption properties of CoFe₂O₄/SWCNTs composites with different experimental parameters. The wave absorption properties of electromagnetic wave-absorbing materials are mainly determined by the complex permittivity ($\epsilon_r = \epsilon' - j\epsilon''$) and complex permeability ($\mu_r = \mu' - j\mu''$), with the real part ϵ' and μ' are related to the ability of the material to store electric field energy and magnetic field energy, respectively, and ϵ'' and μ'' are related to the ability of the material to lose electric field energy and magnetic field energy, respectively [43]. Figure 6a–b shows the real and imaginary parts of the dielectric constants of the prepared CoFe₂O₄/SWCNTs nanocomposites at cobalt salt gradients in the range of 2–18 GHz. The ϵ' and ϵ'' values of the four samples showed a trend of increasing and then gradually decreasing as the content of added cobalt salts increased, indicating that the ϵ' and ϵ'' values did not keep getting larger as the content of cobalt salts increased. The higher ϵ' of the Co-2 sample indicates that the sample has better electromagnetic wave storage and polarization ability. The dielectric tangential loss factor ($\tan\delta_\epsilon = \epsilon'' / \epsilon'$) indicates the dielectric loss capacity of MAM. The $\tan\delta_\epsilon$ of Co-1 gradually increases from 0.21 to 0.6 at 10.4–12.3 GHz. The $\tan\delta_\epsilon$ of Co-4 varied around 0.3. The values of Co-2 reach a maximum peak of 0.73 at 15.4 GHz, and the values of Co-3 reach a maximum peak of 0.65 at 6 GHz. It is proved that the dielectric loss capacity of Co-2 and Co-3 is stronger than that of Co-4 in the frequency range of 2–18 GHz (Figure 6c). In terms of complex permeability, the real part of Co-1 and Co-4 varies around 1.1, and the real part of Co-2 and Co-3 varies around 1.3 (Figure 6d). For the imaginary part of magnetic permeability, Co-2 and Co-3 show a

decrease followed by an increase in the range of 4–8 GHz, while Co-4 shows a regular change around 0.1 and Co-1 decreases from 0.02 to −0.26 at 10.4–12.3 GHz (Figure 6e). The values of the magnetic loss tangent factor ($\tan\delta_\mu = \mu'' / \mu'$) of all four samples in Figure 6f are below 0.25, and the small values indicate that the magnetic storage capacity and magnetic loss capacity are not strong. Taken together, it shows that the CoFe₂O₄/SWCNTs necklace composite has dielectric and magnetic losses, mainly dielectric losses.

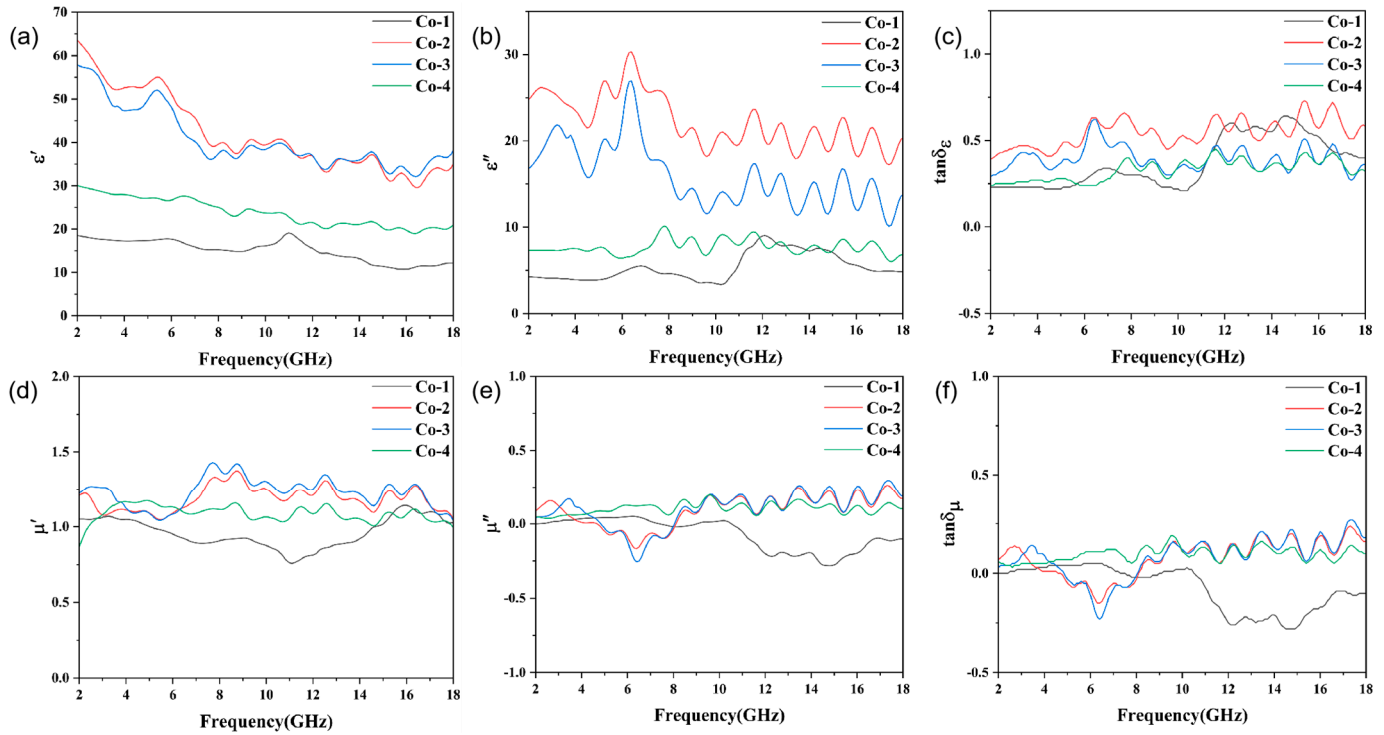


Figure 6. Electromagnetic parameters of Co-1, Co-2, Co-3, Co-4: (a) ϵ' , (b) ϵ'' , (c) dielectric loss angle tangent factor $\tan\delta_\epsilon$, (d) μ' , (e) μ'' , (f) magnetic loss angle tangent factor $\tan\delta_\mu$.

According to the Debye theory, ϵ' and ϵ'' follow Equation (1) [44], where ϵ_∞ and ϵ_s represent the relative permittivity and static permittivity at the high-frequency limit, respectively.

$$(\epsilon' - \frac{\epsilon_s + \epsilon_\infty}{2})^2 + (\epsilon'')^2 = (\frac{\epsilon_s - \epsilon_\infty}{2})^2 \tag{1}$$

Theoretically, one Cole-Cole semicircle corresponds to one Debye relaxation polarization process. As can be seen from Figure 7, the number of Cole-Cole semicircles for the sample with the least amount of cobalt and iron salt addition in the figure is significantly higher than the rest of the samples, probably due to the higher number of CoFe₂O₄ clusters in both samples, which provide more heterogeneous interfaces.

To further explore the absorption performance, we calculated the reflection loss (RL) for different thicknesses in the frequency range from 2 to 18 GHz according to Equations (2) and (3), where Z_{in} is the input impedance of the absorbing material, Z_0 is the impedance in free space, ϵ_r is the complex permittivity, μ_r is the complex permeability, f is the frequency of electromagnetic waves in free space, d is the thickness of the absorber, and c is the speed of light in free space [45].

$$Z_{in} = Z_0 \sqrt{\mu_r / \epsilon_r} \tan h \left[j \left(\frac{2\pi f d}{c} \right) \sqrt{\mu_r \epsilon_r} \right] \tag{2}$$

$$RL(dB) = 20 \log \left| \frac{Z_{in} - Z_0}{Z_{in} + Z_0} \right| \tag{3}$$

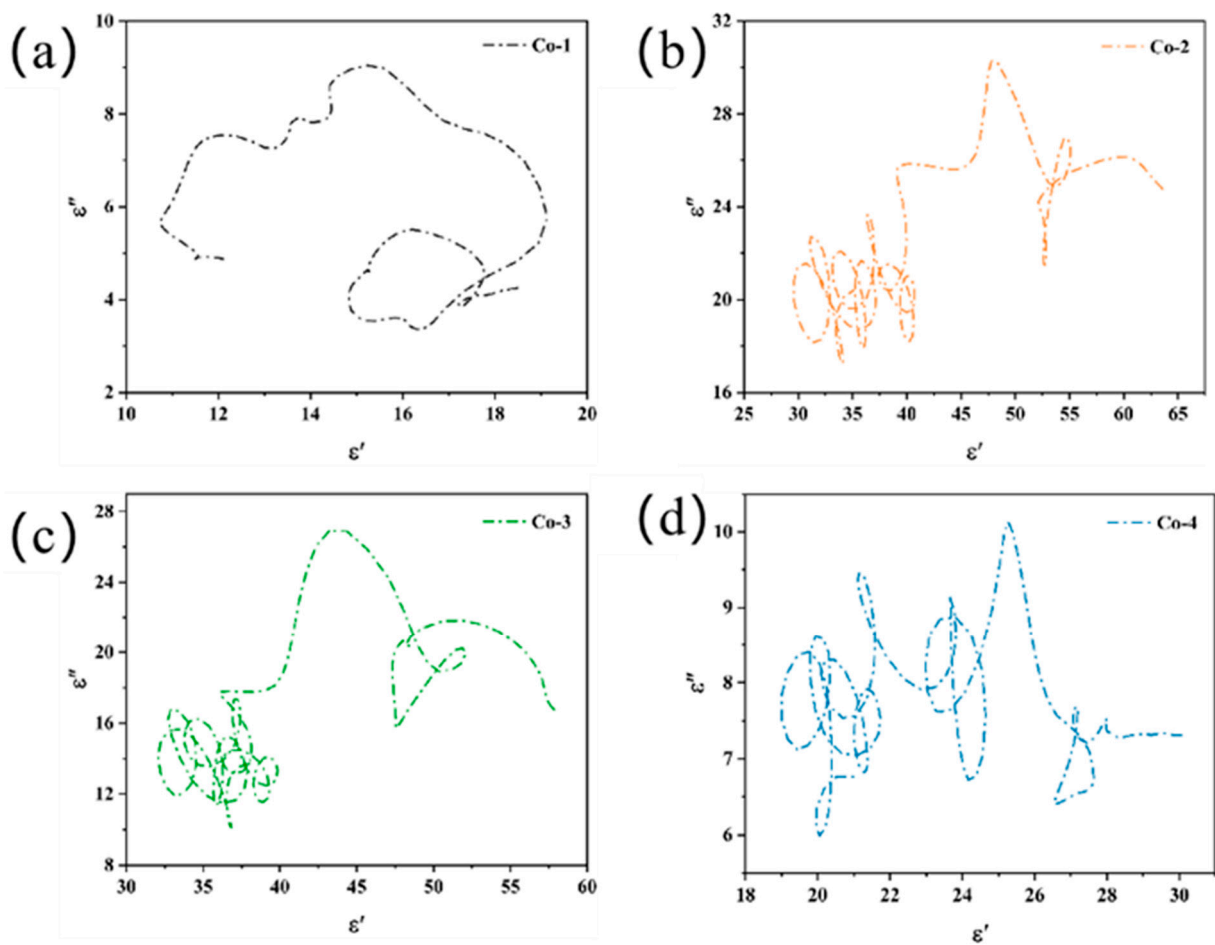


Figure 7. Cole-Cole curves of (a) Co-1, (b) Co-2, (c) Co-3, (d) Co-4.

The data of the four samples were calculated, and a 1.5 mm coating thickness was selected to carry out. The reflection loss (RL) and impedance matching change with frequency was drawn, as shown in Figure 8.

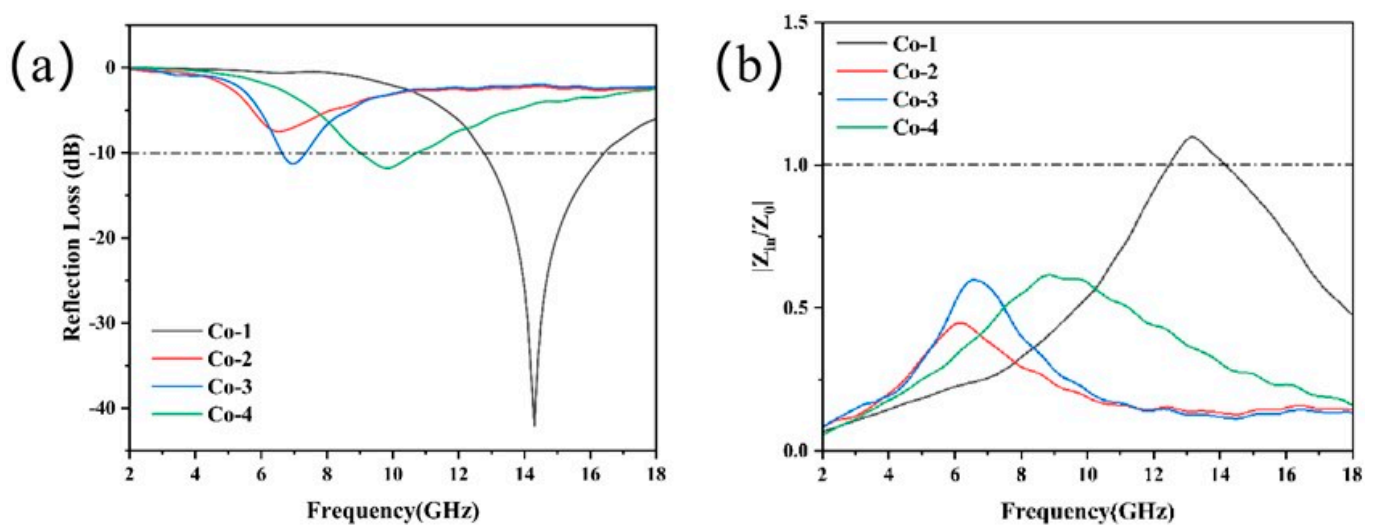


Figure 8. Reflection loss diagram (a) and impedance matching (b) of $\text{CoFe}_2\text{O}_4/\text{SWCNTs}$ heterostructures with different cobalt salt additions at a thickness of 1.5 mm.

From Figure 8a, we can see that with a coating thickness of 1.5 mm, the absorption effect of the Co-1 sample is better, and the peak value of reflection loss reaches -42.07 dB at near 14 GHz. With the increase in cobalt salt addition, the value of reflection loss is -42.07 dB, -7.50 dB, -11.27 dB, and -11.81 dB, and the absorption performance appears to decrease at first and then increase. With the increase in CoFe_2O_4 content, the effective absorption band of the samples shifted to low frequencies, then to high frequencies, when the Co-2 sample reached the lowest frequencies. The results indicate that the CoFe_2O_4 /SWCNTs composites can exhibit excellent microwave absorption performance only when the component ratio is appropriate. The closer the impedance matching Z is to 1, the more the incident wave propagates in the absorbing medium and the better the absorption performance. As can be seen in Figure 8b, Co-1 is closest to 1, so it has the best wave absorption performance.

To further visualize the comparative observation of the absorption capacity of the four samples, three-dimensional plots and contour plots of the relationship between reflection loss, frequency, and sample thickness were drawn, as shown in Figure 9.

As we can see from Figure 9b,f, the Co-2 samples do not exhibit significant microwave absorption properties. None of the RL values reach -10 dB (absorbing 90% of electromagnetic waves) when the range of the thickness of the absorber is 1–5 mm, and the range of frequency of the microwave is 2–18 GHz. When d is 2.09 mm, and f is 4.6 GHz, the minimum RL value of Co-2 is -8.3 dB. As can be seen from Figure 6a–f, Co-2 and Co-3 have extremely similar variations in the parameters of dielectric constant, permeability, dielectric loss factor, and magnetic loss factor. However, since the dielectric constant of Co-3 is lower than that of Co-2, the material impedance matching is improved, and the wave absorption performance is improved. The minimum RL value of Co-3 is -10.52 dB when d is 2.08 mm, and f is 4.9 GHz. The performance of this weak absorption property is consistent with its poorer values of dielectric and magnetic loss factors. In contrast, both Co-1 and Co-4 have good absorption properties. The minimum RL value reaches -42.07 dB (at 14.3 GHz) and EAB of 3.8 GHz (from 12.8 GHz to 16.6 GHz) when the d of Co-1 is 1.50 mm, while when the d of Co-4 is 4.00 mm, the minimum RL value is -19.37 dB and EAB of 0.7 GHz (from 3 GHz to 3.7 GHz). According to Figure 11, the necklace-like CoFe_2O_4 /SWCNTs composites have good absorption capability and low absorption thickness compared with other reported CoFe_2O_4 /CNT composites, but the effective absorption bandwidth is narrow, which limits their practical application capability. However, considering the potential of low-density CoFe_2O_4 /SWCNTs composites in the field of microwave-absorbing materials, this simple and controlled solvothermal method can be extended to composite carbon nanotubes with other ferrites to prepare ferrite/carbon nanotube composites with better microwave absorption properties.

In general, materials with high microwave absorption performance are required to possess low absorber thickness, light mass, wide effective absorption bandwidth, and strong absorption capability. As the requirements for absorbing materials increase, it is clear that a single material cannot meet the requirements for high efficiency, lightweight, and wide efficient absorption bandwidth. In this paper, the samples prepared by simple solvent heat consist of carbon nanotubes as dielectric material and CoFe_2O_4 nanoparticles as magnetic material. Figure 10 shows the magnetization properties of the cobalt salt gradient samples characterized by VSM at room temperature with a magnetic field of $-10,000$ Oe: magnetic hysteresis loops of Co-1, Co-2, Co-3, and Co-4. The saturation magnetization (M_s) of Co-1, Co-2, Co-3, and Co-4 were 70.0, 58.1, 63.4 and 73.5 emu/g, respectively. By increasing the addition of cobalt and iron salts, differences in the degree of crystallization of cobalt ferrite particles and changes in intra-grain defects are produced, causing fluctuations in saturation magnetization. As can be seen from the Co-1 and Co-4 samples in Figure 10, M_s can be enhanced by increasing the magnetic phase. From Figure 10, it was found that the M_s of the samples appeared to decrease and then increase with the increase in the cobalt salt addition ratio, but the difference in the value change was not large. From Figure 3, it can be seen that the size of CoFe_2O_4 microspheres does not vary much, which is in accordance

with the literature expression [46], and the M_s , residual magnetization (M_r), and coercivity (H_c) of nanocrystals are only determined by the size.

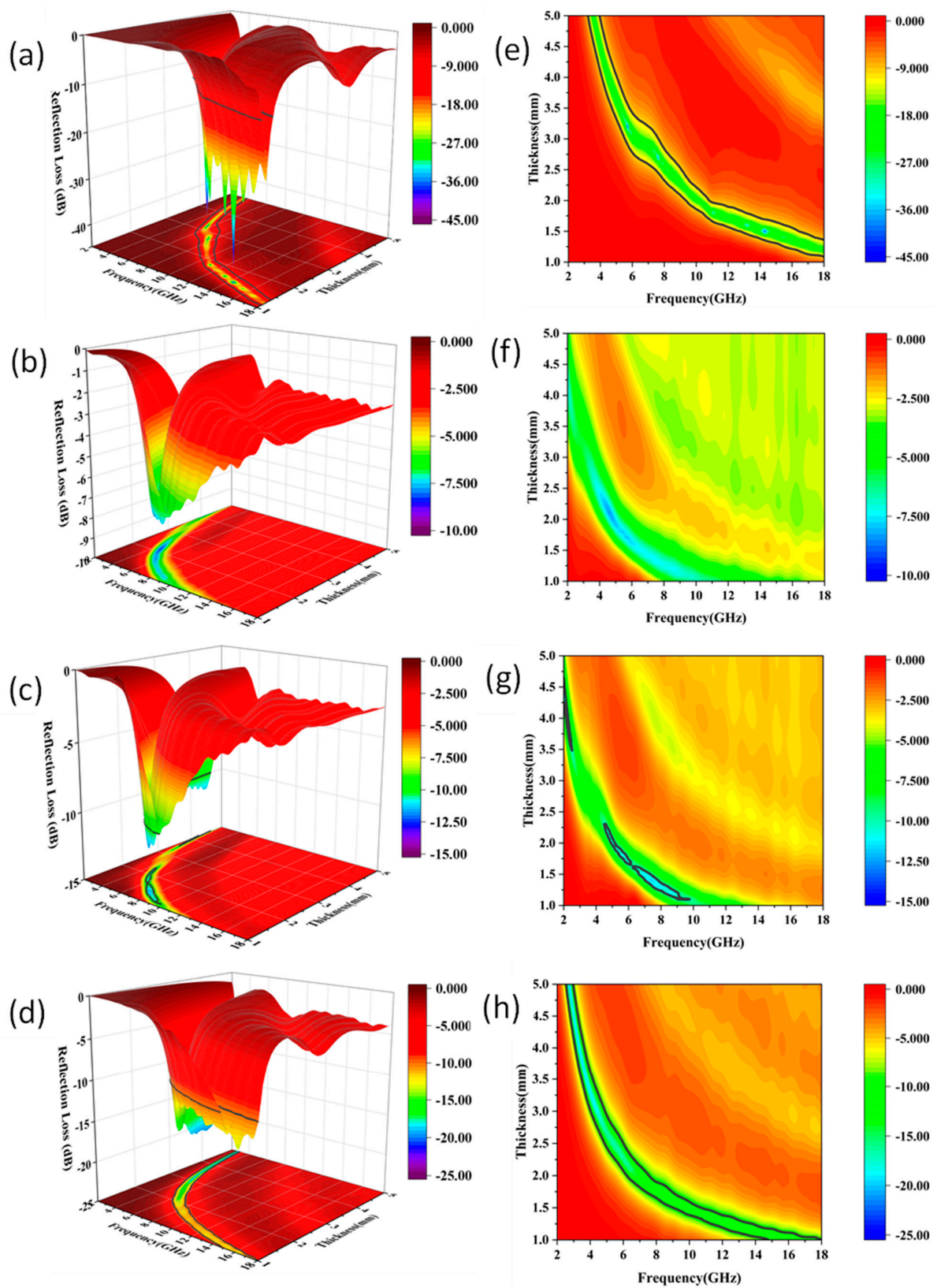


Figure 9. Three-dimensional and contour plots of the RL values of $\text{CoFe}_2\text{O}_4/\text{SWCNTs}$ composites with different cobalt salt contents: (a,e) Co-1, (b,f) Co-2, (c,g) Co-3, and (d,h) Co-4.

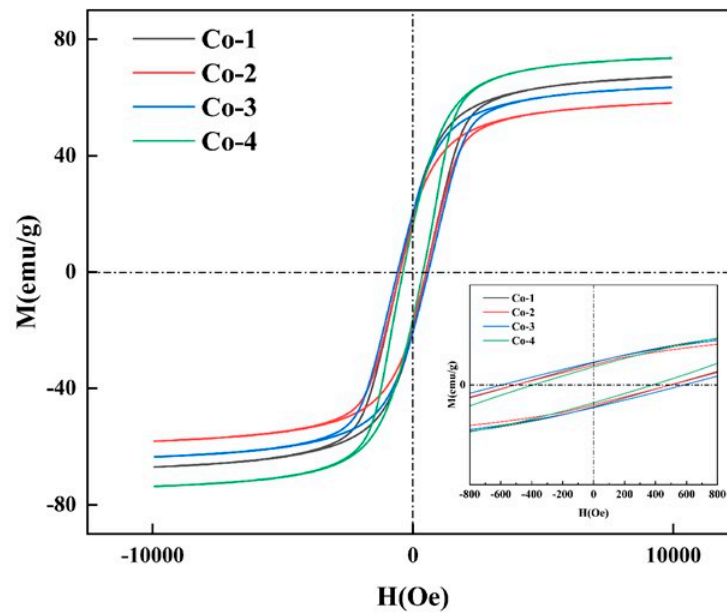


Figure 10. Magnetic hysteresis loops of Co-1, Co-2, Co-3, and Co-4.

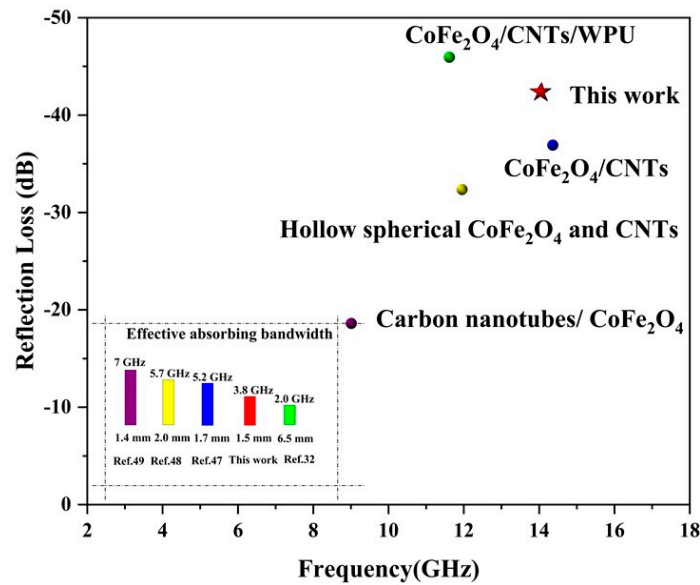


Figure 11. Comparison of the electromagnetic wave absorption capacity of this part of work with some composites of CoFe_2O_4 /carbon [32,47–49].

The microwave absorption performance of CoFe_2O_4 /SWCNTs composites can be attributed to the unique necklace-like structure and the composite loss mechanism of carbon nanotubes and CoFe_2O_4 particles. For pure carbon nanotubes, only dielectric losses contribute to the energy loss of electromagnetic waves, while for pure CoFe_2O_4 particles, the effect of magnetic losses exceeds the dielectric losses. This means that in both cases, the magnetic and dielectric losses are not balanced, which leads to poor wave absorption performance. However, for CoFe_2O_4 /SWCNTs nanocomposites, the microwave absorption is improved due to the combination of paramagnetic CNTs and magnetic CoFe_2O_4 with a better match between dielectric and magnetic losses. Moreover, in addition to defect polarization, dipole polarization, and interfacial polarization, the high impedance matching, and 3D lattice structure allow more electromagnetic waves to enter the absorber (Figure 12), and the CoFe_2O_4 /SWCNTs composites show a large number of nanoparticles anchored on the surface of carbon nanotubes (Figure 3a–d), which provide multiple reflections

in the conductive network with a structure that can effectively dissipate the incident electromagnetic waves. All these play an important role in improving electromagnetic absorption performance.

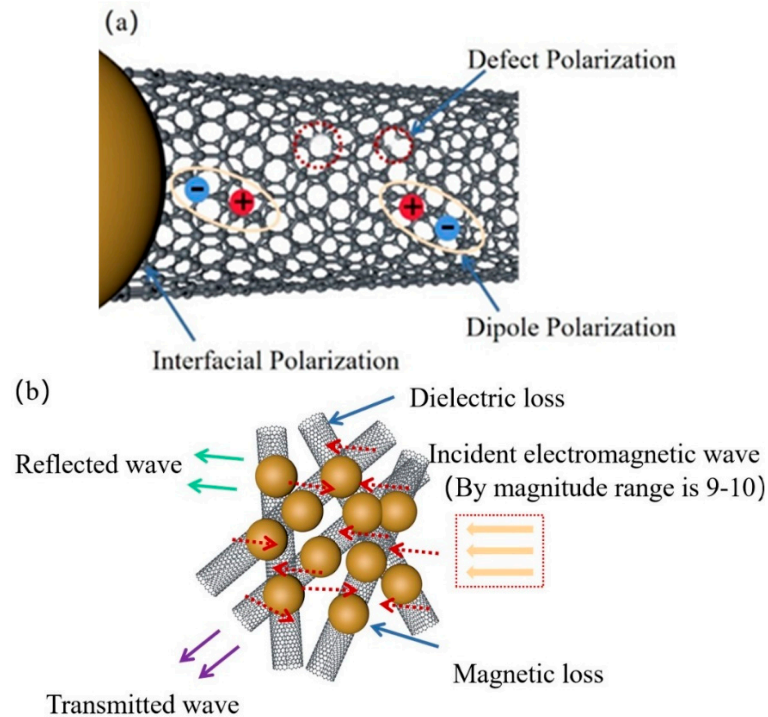


Figure 12. Schematic illustration of EM wave absorption mechanisms for CoFe₂O₄/SWCNTs composites: (a) relaxation loss; (b) absorbing mechanism.

4. Conclusions

In summary, in this work, necklace-like CoFe₂O₄/SWCNTs nanocomposites were prepared by the solvothermal method. This special structural design not only effectively solves the problem of poor impedance matching between a single carbon material and a single ferrite material but also can combine dielectric loss and magnetic loss, which can reflect and scatter electromagnetic waves many times to achieve electromagnetic wave energy dissipation, and as long as good impedance matching is achieved when the component ratio is appropriate. The CoFe₂O₄/SWCNTs nanocomposites exhibit excellent absorption performance: when the additions of FeCl₃·6H₂O, Co(Ac)₂·4H₂O, and NH₄Ac are 0.432 g, 0.200 g, and 0.400 g, respectively, the samples obtained at this time, the best reflection loss reaches −42.07 dB. This simple microstructure design scheme provides a new idea for the preparation of new wave-absorbing materials.

Author Contributions: Conceptualization, M.Z. and X.S.; methodology, S.S.; software, J.W.; validation, M.Z., X.S. and S.S.; formal analysis, M.Z.; investigation, Z.H.; resources, C.L.; data curation, J.G.; writing—original draft preparation, Z.H.; writing—review and editing, M.Z.; visualization, J.G.; supervision, M.Z.; project administration, C.L.; funding acquisition, M.Z. All authors have read and agreed to the published version of the manuscript.

Funding: This research was funded by the National Natural Science Foundation of China (Grant No. 52072063) and the research start-up fund of Foshan Graduate School of Northeastern University.

Institutional Review Board Statement: Not applicable.

Informed Consent Statement: Not applicable.

Data Availability Statement: Not applicable.

Conflicts of Interest: The authors declare no conflict of interest.

References

1. Kong, L.-B.; Li, Z.-W.; Liu, L.; Huang, R.; Abshinova, M.; Yang, Z.-H.; Tang, C.-B.; Tan, P.-K.; Deng, C.-R.; Matitsine, S. Recent progress in some composite materials and structures for specific electromagnetic applications. *Int. Mater. Rev.* **2013**, *58*, 203–259. [[CrossRef](#)]
2. Pan, H.-S.; Cheng, X.-Q.; Zhang, C.-H.; Gong, C.-H.; Yu, L.-G.; Zhang, J.; Zhang, Z. Preparation of Fe₂Ni₂N/SiO₂ nanocomposite via a two-step route and investigation of its electromagnetic properties. *Appl. Phys. Lett.* **2013**, *102*, 012410. [[CrossRef](#)]
3. Wang, B.-L.; Wu, Q.; Fu, Y.-G.; Liu, T. A review on carbon/magnetic metal composites for microwave absorption. *J. Mater. Sci. Technol.* **2021**, *86*, 91–109. [[CrossRef](#)]
4. Yin, P.-F.; Zhang, L.-M.; Feng, X.; Wang, J.; Dai, J.; Tang, Y. Recent Progress in Ferrite Microwave Absorbing Composites. *Integr. Ferroelectr.* **2020**, *211*, 82–101. [[CrossRef](#)]
5. Wang, G.-H.; Ong, S.J.H.; Zhao, Y.; Xu, Z.C.J.; Ji, G.-B. Integrated multifunctional macrostructures for electromagnetic wave absorption and shielding. *J. Mater. Chem. A* **2020**, *8*, 24368–24387. [[CrossRef](#)]
6. Kozlovskiy, A.; Shlimas, D.-I.; Zdorovets, M.-V.; Popova, E.; Elsts, E.; Popov, A.-I. Investigation of the Efficiency of Shielding Gamma and Electron Radiation Using Glasses Based on TeO₂-WO₃-Bi₂O₃-MoO₃-SiO₂ to Protect Electronic Circuits from the Negative Effects of Ionizing Radiation. *Materials* **2022**, *14*, 6071. [[CrossRef](#)]
7. Singh, S.; Kumar, A.; Singh, D. Enhanced Microwave Absorption Performance of SWCNT/SiC Composites. *J. Electron. Mater.* **2020**, *49*, 7279–7291. [[CrossRef](#)]
8. Jian, H.; Du, Q.-R.; Men, Q.-Q.; Guan, L.; Li, R.-S.; Fan, B.-B.; Zhang, X.; Guo, X.-Q.; Zhao, B.; Zhang, R. Structure-dependent electromagnetic wave absorbing properties of bowl-like and honeycomb TiO₂/CNT composites. *J. Mater. Sci. Technol.* **2022**, *109*, 105–113. [[CrossRef](#)]
9. Liao, Q.; He, M.; Zhou, Y.; Nie, S.; Wang, Y.; Hu, S.; Yang, H.; Li, H.; Tong, Y. Highly Cuboid-Shaped Heterobimetallic Metal-Organic Frameworks Derived from Porous Co/ZnO/C Microrods with Improved Electromagnetic Wave Absorption Capabilities. *ACS Appl. Mater. Interfaces* **2018**, *10*, 29136–29144. [[CrossRef](#)]
10. Zhang, F.; Jia, Z.-R.; Wang, Z.; Zhang, C.-H.; Wang, B.-B.; Xu, B.-H.; Liu, X.-H.; Wu, G.-L. Tailoring nanoparticles composites derived from metal-organic framework as electromagnetic wave absorber. *Mater. Today Phys.* **2021**, *20*, 100475.
11. Cao, M.-S.; Yang, J.; Song, W.-L.; Zhang, D.-Q.; Wen, B.; Jin, H.-B.; Hou, Z.-L.; Yuan, J. Ferroferric oxide/multiwalled carbon nanotube vs polyaniline/ferroferric oxide/multiwalled carbon nanotube multiheterostructures for highly effective microwave absorption. *ACS Appl. Mater. Interfaces* **2012**, *4*, 6949–6956. [[CrossRef](#)]
12. Zhao, D.-L.; Shen, Z.-M. Preparation and microwave absorbing properties of microwave absorbing materials containing carbon nanotubes. *J. Inorg. Mater.* **2005**, *20*, 608–612.
13. Huo, J.; Wang, L.; Yu, H. Polymeric nanocomposites for electromagnetic wave absorption. *J. Mater. Sci.* **2009**, *44*, 3917–3927. [[CrossRef](#)]
14. Wu, Y.; Zhao, Y.; Zhou, M.; Tan, S.-J.; Peymanfar, R.; Aslibeiki, B.; Ji, G.-B. Ultrabroad Microwave Absorption Ability and Infrared Stealth Property of Nano-Micro CuS@rGO Lightweight Aerogels. *Nanomicro. Lett.* **2022**, *14*, 171. [[CrossRef](#)] [[PubMed](#)]
15. Peymanfar, R.; Mirkhan, A. Biomass-derived materials: Promising, affordable, capable, simple, and lightweight microwave absorbing structures. *Chem. Eng. J.* **2022**, *446*, 136903. [[CrossRef](#)]
16. Peymanfar, R.; Moradi, F. Functionalized carbon microfibers (biomass-derived) ornamented by Bi₂S₃ nanoparticles: An investigation on their microwave, magnetic, and optical characteristics. *Nanotechnology* **2020**, *32*, 065201. [[CrossRef](#)]
17. Odom, T.W.; Huang, J.L.; Kim, P.; Lieber, C.K. Atomic structure and electronic properties of single-walled carbon nanotubes. *Nature* **1998**, *391*, 62–64. [[CrossRef](#)]
18. Thomassin, J.M.; Jérôme, C.; Pardoën, T.; Bailly, C.; Huynen, I.; Detrembleur, C. Polymer/carbon based composites as electromagnetic interference (EMI) shielding materials. *Mater. Sci. Eng. R Rep.* **2013**, *74*, 211–232. [[CrossRef](#)]
19. Chen, S.-H.; Kuo, W.-S.; Yang, R.-B. Microwave absorbing properties of a radar absorbing structure composed of carbon nanotube papers/glass fabric composites. *Int. J. Appl. Ceram. Technol.* **2019**, *16*, 2065–2072. [[CrossRef](#)]
20. Li, Q.; Xue, Q.-Z.; Zheng, Q.-B.; Hao, L.-Z.; Gao, X.-L. Large dielectric constant of the chemically purified carbon nanotube/polymer composites. *Mater. Lett.* **2008**, *62*, 4229–4231. [[CrossRef](#)]
21. Tang, P.; Zhang, R.; Chen, Z.-Q.; Hu, Y.-P.; Gong, Z.-Z. Dielectric properties of carbon nanotubes-polyethylene composites. *J. Funct. Polym.* **2016**, *29*, 290–295.
22. Wang, L.; Dang, Z.-M. Carbon nanotube composites with high dielectric constant at low percolation threshold. *Appl. Phys. Lett.* **2005**, *87*, 042903. [[CrossRef](#)]
23. Lv, H.-L.; Ji, G.-B.; Zhang, H.-Q.; Du, Y.-W. Facile synthesis of a CNT@Fe@SiO₂ ternary composite with enhanced microwave absorption performance. *RSC Adv.* **2015**, *5*, 76836–76843. [[CrossRef](#)]
24. Xiang, C.-S.; Pan, Y.-B.; Liu, X.-J.; Sun, X.-W.; Shi, X.-M.; Guo, J.-K. Microwave attenuation of multiwalled carbon nanotube-fused silica composites. *Appl. Phys. Lett.* **2005**, *87*, 123103. [[CrossRef](#)]
25. Li, J.-S.; Xie, Y.-Z.; Lu, W.-B.; Chou, T.-W. Flexible electromagnetic wave absorbing composite based on 3D rGO-CNT-Fe₃O₄ ternary films. *Carbon* **2018**, *129*, 76–84. [[CrossRef](#)]
26. Wu, G.; He, Y.; Zhan, H.; Shi, Q.-Q.; Wang, J.-N. A novel Fe₃O₄/carbon nanotube composite film with a cratered surface structure for effective microwave absorption. *J. Mater. Sci. Mater. Electron.* **2020**, *31*, 11508–11519. [[CrossRef](#)]

27. Zhang, M.; Song, S.-N.; Liu, Y.-M.; Hou, Z.-X.; Tang, W.-Y.; Li, S.-N. Microstructural Design of Necklace-Like Fe₃O₄/Multiwall Carbon Nanotube (MWCNT) Composites with Enhanced Microwave Absorption Performance. *Materials* **2021**, *14*, 4783. [[CrossRef](#)]
28. Sharifianjazi, F.; Moradi, M.; Parvin, N.; Nemati, A.; Rad, A.J.; Sheysi, N.; Abouchenari, A.; Mohammadi, A.; Karbasi, S.; Ahmadi, Z.; et al. Magnetic CoFe₂O₄ nanoparticles doped with metal ions: A review. *Ceram. Int.* **2020**, *46*, 18391–18412. [[CrossRef](#)]
29. Klym, H.; Karbovnyk, I.; Luchechko, A.; Kostiv, Y.; Pankratova, V.; Popov, A.-I. Evolution of Free Volumes in Polycrystalline BaGa₂O₄ Ceramics Doped with Eu³⁺ Ions. *Crystals* **2022**, *11*, 1515. [[CrossRef](#)]
30. Zhao, D.; Wu, X.; Guan, H.; Han, E. Study on supercritical hydrothermal synthesis of CoFe₂O₄ nanoparticles. *J. Supercrit. Fluids* **2007**, *42*, 226–233. [[CrossRef](#)]
31. Fu, M.; Jiao, Q.-Z.; Zhao, Y.; Li, H.-S. Vapor diffusion synthesis of CoFe₂O₄ hollow sphere/graphene composites as absorbing materials. *J. Mater. Chem. A* **2014**, *2*, 735–744. [[CrossRef](#)]
32. Luo, J.-W.; Wang, Y.; Qu, Z.-J.; Wang, W.; Yu, D. Lightweight and robust cobalt ferrite/carbon nanotubes/waterborne polyurethane hybrid aerogels for efficient microwave absorption and thermal insulation. *J. Mater. Chem. C* **2021**, *9*, 12201–12212. [[CrossRef](#)]
33. Zhang, S.-L.; Jiao, Q.-Z.; Zhao, Y.; Li, H.-S.; Wu, Q. Preparation of rugby-shaped CoFe₂O₄ particles and their microwave absorbing properties. *J. Mater. Chem. A* **2014**, *2*, 18033–18039. [[CrossRef](#)]
34. Wu, M.; Darboe, A.K.; Qi, X.-S.; Xie, R.; Qin, S.-J.; Deng, C.-Y.; Wu, G.-L.; Zhong, W. Optimization, selective and efficient production of CNTs/Co_xFe_{3-x}O₄ core/shell nanocomposites as outstanding microwave absorbers. *J. Mater. Chem. C* **2020**, *8*, 11936–11949. [[CrossRef](#)]
35. Peymanfar, R.; Selseleh-Zakerin, E.; Ahmadi, A. Tailoring energy band gap and microwave absorbing features of graphite-like carbon nitride (g-C₃N₄). *J. Alloys Compd.* **2021**, *867*, 159039. [[CrossRef](#)]
36. Chen, G.; Zhang, L.-M.; Luo, B.-C.; Wu, H.-J. Optimal control of the compositions, interfaces, and defects of hollow sulfide for electromagnetic wave absorption. *J. Colloid Interf. Sci.* **2021**, *607*, 24–33. [[CrossRef](#)]
37. Chen, T.; Du, P.; Jiang, W.; Liu, J.; Hao, G.-Z.; Gao, H.; Xiao, L.; Ke, X.; Zhao, F.-Q.; Xuan, C.-L. A facile one-pot solvothermal synthesis of CoFe₂O₄/RGO and its excellent catalytic activity on thermal decomposition of ammonium perchlorate. *RSC Adv.* **2016**, *6*, 83838–83847. [[CrossRef](#)]
38. Yu, M.; Feng, Z.-H.; Huang, Y.; Wang, K.; Liu, L. CoFe₂O₄ nanoparticles directly grown on carbon nanotube with coralline structure as anodes for lithium ion battery. *J. Mater. Sci. Mater. Electron.* **2019**, *30*, 4174–4183. [[CrossRef](#)]
39. Wang, C.-X.; Wang, B.-B.; Cao, X.; Zhao, J.-W.; Chen, L.; Shan, L.-G.; Wang, H.-N.; Wu, G.-L. 3D flower-like Co-based oxide composites with excellent wideband electromagnetic microwave absorption. *Compos. B. Eng.* **2021**, *205*, 108529. [[CrossRef](#)]
40. Zhou, C.-H.; Wu, C.; Yan, M. Hierarchical FeCo@MoS₂ Nanoflowers with Strong Electromagnetic Wave Absorption and Broad Bandwidth. *ACS Appl. Nano Mater.* **2018**, *1*, 5179–5187. [[CrossRef](#)]
41. Guo, D.-G.; Kang, H.-Z.; Wei, P.-K.; Yang, Y.; Hao, Z.-W.; Zhang, Q.-X.; Liu, L. A high-performance bimetallic cobalt iron oxide catalyst for the oxygen evolution reaction. *CrystEngComm* **2020**, *22*, 4317–4323. [[CrossRef](#)]
42. Sun, X.; Zhu, X.-Y.; Yang, X.-F.; Sun, J.; Xia, Y.-Z.; Yang, D.-J. CoFe₂O₄/carbon nanotube aerogels as high performance anodes for lithium ion batteries. *Green Energy Environ.* **2017**, *2*, 160–167. [[CrossRef](#)]
43. Hasar, U.C. A New Microwave Method Based on Transmission Scattering Parameter Measurements for Simultaneous Broadband and Stable Permittivity and Permeability Determination. *Electromagn. Waves* **2009**, *93*, 161–176. [[CrossRef](#)]
44. Han, M.-Y.; Zhou, M.; Wu, Y.; Zhao, Y.; Cao, J.-M.; Tang, S.-L.; Zou, Z.-Q.; Ji, G.-B. Constructing angular conical FeSiAl/SiO₂ composites with corrosion resistance for ultra-broadband microwave absorption. *J. Alloys Compd.* **2022**, *902*, 163792. [[CrossRef](#)]
45. Wang, S.-S.; Zhu, H.-H.; Jiao, Q.-Z.; Jiao, X.-G.; Feng, C.-H.; Li, H.-S.; Shi, D.-X.; Wu, Q.; Zhao, Y. Controllable synthesis of multi-shelled SiO₂@C@NiCo₂O₄ yolk-shell composites for enhancing microwave absorbing properties. *New J. Chem.* **2021**, *45*, 20928–20936. [[CrossRef](#)]
46. Song, Q.; Zhang, Z.-J. Shape Control and Associated Magnetic Properties of Spinel Cobalt Ferrite Nanocrystals. *J. Am. Chem. Soc.* **2004**, *126*, 6164–6168. [[CrossRef](#)]
47. Yuan, Y.; Wei, S.-C.; Liang, Y.; Wang, B.; Wang, Y.-J.; Xin, W.; Wang, X.-L.; Zhang, Y. Solvothermal assisted synthesis of CoFe₂O₄/CNTs nanocomposite and their enhanced microwave absorbing properties. *J. Alloys Compd.* **2021**, *867*, 159040. [[CrossRef](#)]
48. Zhang, S.-L.; Qi, Z.-W.; Zhao, Y.; Jiao, Q.-Z.; Ni, X.; Wang, Y.-J.; Chang, Y.; Ding, C. Core/shell structured composites of hollow spherical CoFe₂O₄ and CNTs as absorbing materials. *J. Alloys Compd.* **2017**, *694*, 309–312. [[CrossRef](#)]
49. Che, R.-C.; Zhi, C.-Y.; Liang, C.-Y.; Zhou, X.-G. Fabrication and microwave absorption of carbon nanotubes/CoFe₂O₄ spinel nanocomposite. *Appl. Phys. Lett.* **2006**, *88*, 033105. [[CrossRef](#)]